

therapeutic temperatures for tumour ablation can be achieved with a less concentrated MNP dispersion, thereby reducing the dose needed. Nevertheless, due to the nano-sized crystals, the -Fe₃N is air sensitive, which results in massive oxidation. Thus, a robust surface protection must be realised. While considering the potential biomedical applications, we propose a silica encapsulation procedure to hinder -Fe₃N oxidation and to establish biocompatibility, together with possibility to form aqueous dispersions. To successfully grow a silica layer, we have chosen a route of -Fe₃N surface passivation, which we present in this contribution, together with insight into magnetic behaviour of complex core@shell MNPs. The bright-field transmission electron microscope micrographs (Figure 1: A) and small-angle X-ray scattering (Figure 1: B) show well-defined core@shell MNP morphology of the passivated nanoparticles with a mean particle diameter of 17.2(2) nm. Nevertheless, the macroscopic magnetization measurements revealed unexpected behaviour leading to a decrease in saturation magnetization and the presence of exchange bias at 5 K. To further explore, the complex magnetic nature of this material was disentangled by probing magnetic scattering fluctuations using the magnetic small-angle neutron scattering with incident beam polarization at the D33 instrument at ILL [2]. Finally, we will disentangle the magnetic morphology contributions from the magnetic core and shell part of passivated -Fe₃N MNPs and discuss the resulting magnetic response of the presented MNPs in detail.

- I. Dirba et al., J. Phys. D: Appl. Phys, 56, 025001 (2023). doi: 10.1088/1361-6463/aca0a9.
- Š. Hricov et al., Unmasking the Complex Core-Multishell Morphology of Magnetic Nanoparticles. Institut Laue-Langevin, proposal No. DIR-297 (2023). doi: 10.5291/ILL-DATA.DIR-297

This work was supported by the Czech Science Foundation (22-10035K) and the AMULET project, co-funded by MŠMT and the EU (CZ. 02.01.01/00/22_008/0004558). We also acknowledge the Institut Laue-Langevin for beamtime and financial support.

Session XII - September 11, Thursday

L43

LAUEDB: A DATASET FOR LAUE PATTERNS

Štěpán Venclík, Tomáš Červeň, Jan Kříž, David Sviták, Petr Čermák

Charles University, Prague, Czech Republic

Laue diffraction is a widely used technique for orienting single crystals and a routine procedure during sample preparation for many scientists. Over the years, a variety ofsoftware tools have been developed to assist in interpreting Laue patterns [1, 2]. Despite significant progress in image processing and pattern recognition, a robust and fully automated solution for indexing Laue patterns has yet to be achieved.

In recent years, **machine learning** has emerged as a promising approach to tackle this challenge [3]. However, the development and validation of more advanced algorithms are currently hindered by the lack of annotated experimental datasets. As a result, all training and testing are still conducted exclusively on synthetic data.

LaueDB aims to bridge this gap by creating a dataset of oriented X-ray and neutron Laue patterns that could

serve as a training and evaluation dataset for both classical and machine learning approaches.

We plan to utilise the Automatic Laue Sample Aligner (ALSA) [4] to create the initial dataset, capturing a large number of patterns for each sample crystal, as well as collaborate with research infrastructures to develop a submission pipeline for patterns created during routine sample orientation. In addition, existing tools and algorithms for peak finding and Laue indexing will be compared.

- 1. Esmeralda Laue Suite (https://code.ill.fr/scientific-software/esmeralda).
- 2. Clip4 (https://clip4.sourceforge.net/)
- Purushottam Raj Purohit, R. R. P., Tardif, S., Castelnau, O., Eymery, J., Guinebretiere, R., Robach, O., Ors, T. & Micha, J.-S. (2022). J. Appl. Cryst. 55, 737-750.
- 4. ALSA (https://charlesautomata.cz/alsa).



L44

PSB_GUI – MATLAB ROUTINE FOR THE REFINEMENT OF RESIDUAL STRESSES, MICROSTRAIN AND CRYSTALLITE SHAPE IN CUBIC MATERIALS

Petr Cejpek^{1,2}, David Rafaja²

¹Institute of Physics, Czech Academy of Sciences, Na Slovance 1999/2, 182 00 Praha 8, Czech Republic ²Institute of Materials Science, TU Bergakademie Freiberg, Gustav-Zeuner-Str. 5, 09599 Freiberg, Germany

Residual stress is commonly determined from the shift of X-ray diffraction (XRD) lines using the of sin² method. Microstrain and grain sizes are typically evaluated from the line broadening and Williamson-Hall plot. This standard procedure is mainly applied to polycrystalline materials or thin films. Regarding grain or crystallite shapes, the spherical shape is usually sufficient enough.

However, in many cases, more complex theoretical models are required to achieve a reasonable fit of the experimental data. Moreover, such situations can occur even in relatively simple systems like thin Mo film deposited on single-crystalline MgO(100) substrate [1]. As the result of the minimisation of deformation energy, Mo forms a hetero-epitaxially grown matrix along with the twins that are specifically oriented with respect the Mo matrix. Therefore, the approach related to the family of crystallites method [2] needs to be applied during the refinement. This requires the experimental data correctly separated into groups and the diffraction peaks need to be precisely indexed. Each group is then assigned to different theoretical models for XRD line shift and broadening refinement, since the different families of crystallites can exhibit different properties. For example, different components of the residual stress or asymmetric shapes of crystallites grown in the specific crystallographic directions.

For this purpose, the Matlab routine *PSB_GUI* (with a graphical user interface) has been developed. It enables a complex refinement of XRD line shift and broadening for cubic materials. The routine allows the separation of the datapoints into groups and each of these groups can be as-

sociated with its own unique combination of theoretical models for residual stress, microstrain and grain sizes. For XRD line shift refinement, the following models are supported: Voigt, Reuss, Vook-Witt, stress factors for textured polycrystals or the possibility to refine individual stress components. [3] For the line broadening, models include spherical crystallites, cylindrical and ellipsoidal crystallites grown in specific crystallographic directions, stacking faults, isotropic microstrain, and anisotropic microstrain connected to dislocations [4] or specific directions of Burgers vectors.

To run *PSB_GUI* properly, Matlab along with the Optimalisation toolbox is required. The entire routine is currently available on GitHub at the following link: https://github.com/PetrCejpek/PSB_GUI.

- 1. Cejpek, P., et al. Lattice strain relaxation in thin Mo films grown heteroepitaxially on MgO single crystals, Journal of Applied Crystallography, under review.
- 2. Kužel, R., et al. Complex XRD microstructural studies of hard coatings applied to PVD-deposited TiN films. Part I: Problems and methods, Thin Solid Films **247** (1994), 64–78, https://doi.org/10.1016/0040-6090(94)90477-4.
- Welzel, U., et al. Stress analysis of polycrystalline thin films and surface regions by X-ray diffraction, Journal of Applied Crystallography 38 (2005), 1–29, https://doi.org/10.1107/S0021889804029516.
- Ungár, T., et al. The contrast factors of dislocations in cubic crystals: the dislocation model of strain anisotropy in practice, Journal of Applied Crystallography 32(5) (1999), 992–1002, https://doi.org/10.1107/S0021889899009334.

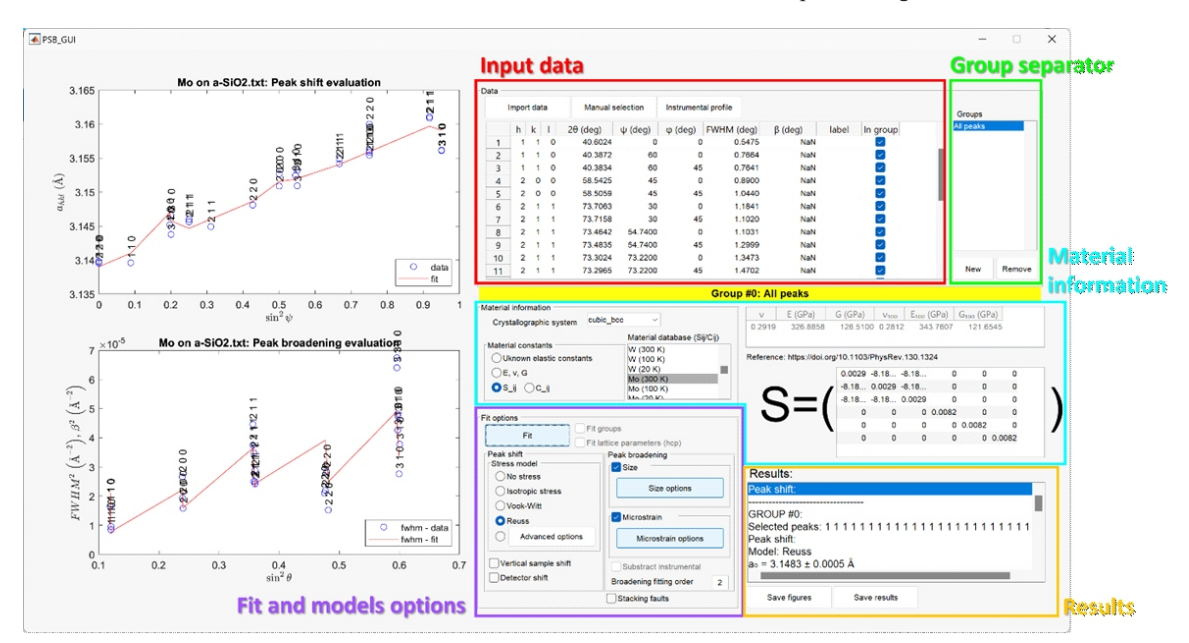


Figure 1. Overview of the PSB GUI main window.



L45

EFFECTS OF HEAT TREATMENT ON MICROSTRUCTURE, PORE MORPHOLOGY, AND MICROMECHANICAL PROPERTIES OF AM-PRODUCED TIGAL4V ALLOY

Ubaid Ahmed^{1,2} A. Bhardwaj¹, Miroslav Lebeda¹, J. Kopeček¹, Daniel Šimek¹

¹FZU, Institute of Physics of the Czech Academy of Sciences, Na Slovance 2, Prague 8, 182 21, Czech Republic

²Department of Condensed Matter Physics, Charles University, Prague, Czech Republic

Ti6Al4V, a grade 5 titanium alloy, is widely utilized in aerospace, biomedical, marine, and energy sectors due to its high strength-to-weight ratio, superior corrosion resistance, and excellent biocompatibility. With the advent of advanced manufacturing techniques such as Additive Manufacturing (AM), the production of intricate geometries has become more efficient compared to traditional methods. However, the localized thermal gradients generated during AM processes significantly influence the microstructure, pore morphology, and mechanical properties of the material. This study investigates the effects of heat treatment on the microstructure, pore morphology, and micromechanical properties of AM-produced Ti6Al4V specimens.

Using Micro-Computed Tomography (Micro CT) and X-ray Diffraction (XRD), pore defect volumes, distributions, equivalent spherical diameters, and sphericity coefficients were analysed under three heat treatment

conditions (550 °C, 750 °C, and 1150 °C). The average pore volumes were found to be 1.975×10^{-4} mm³, 1.2838×10^{-4} mm³, and 4.347×10^{-5} mm³ for the as-cast and heat-treated samples at 550 °C, 750 °C, respectively. The mean sphericity values were 0.747, 0.749, and 0.921, indicating improved pore uniformity and shape at 750°C.

Hardness measurements revealed values up to 7.17 GPa, while the reduced modulus values up to 139.57 GPa. The results demonstrate that annealing at 750 °C achieved the most favourable balance between reduced pore volume and uniformity, attributed to stabilization of the alpha phase and atomic diffusion minimizing surface energy. Additionally, at this temperature, the mechanical properties were improved, providing a balance between strength and elasticity. These findings highlight the potential of heat treatment optimization to enhance the performance of AMproduced Ti6Al4V for demanding applications.

L46

Microstructure of rotary swaged copper bars with carbon admission

MIKROSTRUKTURA MĚDĚNÝCH, ROTAČNĚ KOVANÝCH TYČÍ S PŘÍMĚSÍ UHLÍKATÉ FRAKCE

J. Kopeček^{1*}, L. Kunčická², T. Kmječ¹, J. Walek², D. Šimek¹, U. Ahmed¹, J. Duchoň¹, A. Bhardwaj¹ and R. Kocich²

¹FZU – Institute of Physics of the Czech Academy of Sciences, Praha, Czech Republic, ²Faculty of Materials Science and Technology, VŠB–Technical University of Ostrava, Ostrava-Poruba, Czech Republic

Jednou z hlavních aplikačních oblastí mědi jsou elektrické vodiče, což je odrazem jejích výborných vodivostních vlastností [1]. Náležitě čistá a vyžíhaná měď má excelentní vodivost, která však klesá vlivem příměsových atomů, stejně jako vlivem plastické deformace. Přesto byla pozorována výborná vodivost materiálů připravených některými metodami značné plastické deformace, které vedou k tvorbě nanodvojčat [2]. Jednou z metod, kterou je možné připravit takovou mikrostrukturu je rotační kování [3].

V prezentované práci se věnujeme materiálům připraveným kompaktizací prášku se sférickými zrníčky a příměsí uhlíkaté fáze deponované na povrch prášků. Koncept vychází z předchozích experimentů s kováním kompaktní čisté mědi [4,5] a materiálů připravených kompaktizací prášků s příměsí oxidů [6]. Elektrické vodivost takto připravených materiálů v ose kování

přesahuje vodivost konvenčně žíhané mědi IACS (International Annealed Copper Standard).

Vykované tyče připravené na VŠB – TU Ostrava byly použity pro přípravu metalografických vzorků, případně dále žíhány a všechny stavy byly standardně zkoumány pomocí SEM (Tescan FERA 3), EDS a EBSD (EDAX Octane super 60 mm² a Digiview IV), TEM (Jeol JEOL 2000 FX) a XRD (Panalytical X´Pert). Pro vyhodnocení mikrostruktury pomocí EBSD byl použit software OIM 9 využívající sférických harmonických funkcí pro určení orientace krystalové mříže.

Potvrdili jsme, že rotační kování prášků s obsahem uhlíkaté fáze vede ke vzniku textury s komponentami 100 a 111 v ose kování, což je podobné chování jaké bylo pozorováno u kování při teplotě kapalného dusíku, které vytváří silnou texturu ve směru 111 v ose kování, složka



ve směru (100) je oproti čistému materiálu výrazně slabší. Zrna jsou ve směru osy tyče protažena, ale jsou významně kratší než v kovaném materiálu. Pomocí TEM byly pozorovány dislokace v kovaném materiálu, avšak nikoli precipitáty. Zaměřili jsme se také na směrovou závislost elektrické vodivosti vzhledem k osám kování.

- J. R. Davies (Ed), ASM Specialty Handbook, Copper and Copper Alloys, Materials Park, ASM International, 2001.
- L. Lu, Y.F. Shen, X.H. Chen, L.H. Qian, K. Lu, Ultrahigh strength and high electrical conductivity in copper, Science, 304 (2004), 422-426.
- 3. X. Ke, J. Ye, Z. Pan, J. Geng, M.F. Besser, D. Qu, A. Caro, J. Marian, R.T. Ott, Y.M. Wang, F. Sansoz, Ideal maximum strengths and defect-induced softening in

- nanocrystalline-nanotwinned metals, Nature Materials, 18 (2019), 1207-1214.
- 4. J. Kopeček, L. Bajtošová, P. Veřtát, D. Šimek, (Sub)structure Development in Gradually Swaged Electroconductive Bars, Materials, 16 (2023) 5324-1 5324-12.
- R. Kocich, L. Kunčická, Crossing the limits of electric conductivity of copper by inducing nanotwinning via extreme plastic deformation at cryogenic conditions, Mat. Char. 207 (2024) 113513.
- L. Kunčická, J. Walek, R. Kocich, Deformation Behavior of La₂O₃-Doped Copper during Equal Channel Angular Pressing, Adv. Eng. Mater. (2024) 2402412.

We acknowledge Czech Science Foundation project 25-16860S and CzechNanoLab Research Infrastructure (LM2023051) by MEYS CR support.

Session XIII - September 12, Friday

L47

Y-HEXAFERRITE THIN FILMS DEPOSITED BY CHEMICAL SOLUTION DEPOSITION ON DIFFERENT SUBSTRATES STUDIED BY XRD

Radomír Kužel¹, Milan Dopita¹, Lukáš Horák¹, Josef Buršík²

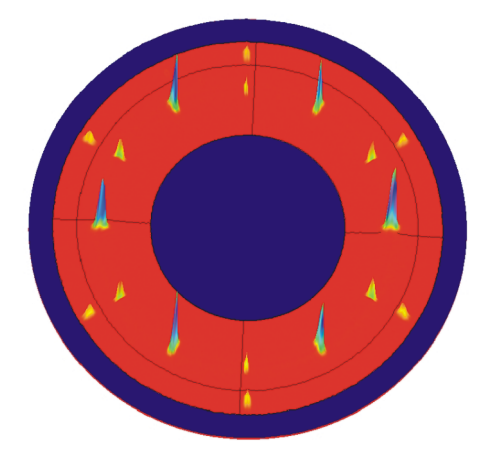
¹Charles University, Faculty of Mathematics and Physics, Ke Karlovu 5, Praha 2 121 16, Czech Republic, ²Institute of Inorganic Chemistry of the Czech Academy of Sciences, v.v.i., Husinec-Řež 1001, 250 68, Czech Republic

radomir.kuzel@matfyz.cuni.cz

Thin films of several phases of hexagonal ferrites with a potential of magnetoelectric effect (ME) were prepared by a chemical solution deposition method, and the number of processing parameters was tested and optimized with the of minimizing the amount of impurities that could spoil the magnetic properties of the final material. With the aim of preparation of highly oriented ferrite films, several substrates were used, and different substrate/seeding layer/ferrite layer architectures were proposed. [1-5].

The mechanism of ME in Y-type hexaferrite films appears to be significantly influenced by lattice parameters.

New Y-ferrite phases were prepared with the composition $Ba_xSr_{2-x}Co_2Fe_{11.1}Al_{0.9}O22$, and it was found that the magnetic structure is non-colinear ferrimagnetic type. These films could be prepared with good out-of-plane and in-plane orientation directly on STO - SrTiO (111) substrate, but the M-phase seeding layer usually leads to better results. The ME effect was identified to be maximum for equal content of barium and strontium but the dependence on x is now studied in more detail. In the project, we investigate the influence of the degree and type of preferred orientation of the films as well as their real structure on the



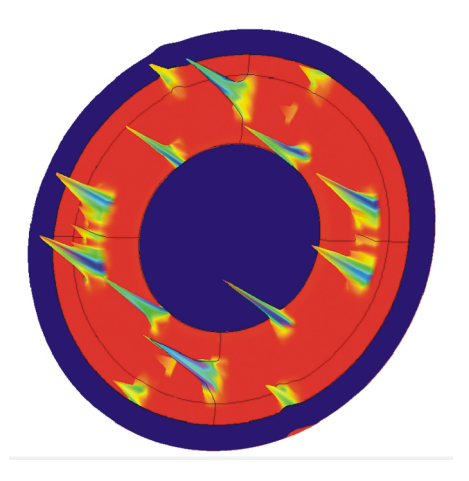


Figure 1. Illustrations of preferred orientation of Y-films. Partial pole figures (119) for the film grown on $MgAl_2O_4$ (111) substrate (left), and (024) for the film grown on Al_2O_3 *a*-cut.



ME effect. By using different substrates, different preferred orientations and strains can be obtained.

Symmetrical θ – θ scans often indicated a strong preferred orientation (000*l*) on STO (111). This is the so-called out-of-plane orientation. In case of fiber texture, its degree can be well characterized by the ω scans (rocking curves). For the estimation of the alignment of planes perpendicular to the substrate, measurement of additional asymmetric Bragg reflections is necessary, simply by the ϕ scans (rotation on the axis perpendicular to the film plane). The lattice parameters of the films were obtained by evaluating the maxima positions of about 30 diffraction profiles measured at different sample inclinations and \ddot{o} angles corresponding to the maxima, i.e., by creating a powder-like pattern [6].

Several sets of Y-films were investigated. Films with different thicknesses were deposited on the STO substrate with orientations (111), (110), (100), and ceramics. In all cases, (00*l*) textures of Y-phases of different degrees were observed but only for (111) also a strong (111) texture was detected, as it can be expected. Then other substrates were used - MgO (111), LaAlO₃ (111) - LAO, stabilized cubic zirconia (ZrO₂) and MgAl₂O₄ (111). In this case, significant out-of-plane and in-plane orientations of Y-films were observed for LAO substrates with FWHMs of both ω and $\ddot{\odot}$ scans of approximately 0.4°. For MgO substrates both orientations were also indicated with a slightly wider FWHMs (over 1°). On zirconia, the preferred orientations are relatively poor with clear domains in in-plane orientations. An-

other set of substrates used were differently oriented sapphire substrates (rhombohedral Al_2O_3) – c-cut (000l), a-cut (11-20), m-cut(10-10), r-cut (1-120). It seems that different pronounced textures of Y-hexaferrites can grow there including the (h00) orientation on a-cut of substrate, or (hh0) on m-cut of substrate. Some illustrations of preferred orientation with a few domains are shown in Fig. 1.

- Shin, KW; Soroka, M.; Shahee, A; Kim, KH; Buršík, J.; Kužel, R; Vronka, M; Aguirre, MH: Advanced Electronic Materials. v. 8 (2022). 2101294.
- J. Buršík, R. Uhrecký, D. Kaščáková, M. Slušná, M. Dopita, R. Kužel, *Journal of the European Ceramic Society* 36 (2016) 3173–3183.
- R. Uhrecký, J. Buršík, M. Soroka, R. Kužel, J. Prokleška, Thin Solid Films. 622 (2017) 104–110.
- M. Soroka, J. Buršík, R. Kužel, J. Prokleška, M.H. Aquirre, *Thin Solid Films*, 726 (2021) 138670.
- M. Soroka, J. Buršík, R. Kužel, L. Horák, J. Prokleška, M. Vronka & V. Laguta. *Journal of European Ceramic Society*. 43, (2023) 6916-6924.
- R. Kužel, J. Buršík, M. Dopita, L. Horák, M. Soroka, Materials Structure 30 (2024) 328-331.

The authors appreciate the support by the grant of the Czech Grant Agency, no. 24-12710S.